

Phase separation effects in charge-ordered $\text{Pr}_{0.5}\text{Ca}_{0.5}\text{MnO}_3$ thin film

S. de Brion, G. Storch, G. Chouteau, A. Janossy, and W. Prellier, E. Rauwel Buzin

(Dated: August 26, 2018)

Compressed $\text{Pr}_{0.5}\text{Ca}_{0.5}\text{MnO}_3$ films (250nm) deposited on LaAlO_3 have been studied by Electron Spin Resonance technique under high frequency and high magnetic field. We show evidences for the presence of a ferromagnetic phase (FM) embedded in the charge-order phase (CO), in form of thin layers which size depends on the strength and orientation of the magnetic field (parallel or perpendicular to the substrate plane). This FM phase presents an easy plane magnetic anisotropy with an anisotropy constant 100 times bigger than typical bulk values. When the magnetic field is applied perpendicular to the substrate plane, the FM phase is strongly coupled to the CO phase whereas for the parallel orientation it keeps an independent ferromagnetic resonance even when the CO phase becomes antiferromagnetic.

PACS numbers:

I. INTRODUCTION

In the past few years the charge-ordering (CO) phenomena¹ attracted much attention. This feature is observed in compounds like e.g. $\text{Pr}_{0.5}\text{Ca}_{0.5}\text{MnO}_3$ ^{2,3} electrons become localized due to the ordering of heterovalent cations in two different sublattices with Mn^{3+} and Mn^{4+} ions respectively. The materials are insulating below the CO transition temperature (T_{CO}), but it is possible to melt the CO state and render the material ferromagnetic and metallic (FM state) by, for example, the application of a magnetic field. In $\text{Pr}_{0.5}\text{Ca}_{0.5}\text{MnO}_3$ this critical magnetic field is around 25T at 4K. One of the open questions which has attracted much attention recently is the possibility of a coexistence of two phases⁴ i.e. the ferromagnetic metallic phase (FM) and the charge-order insulating (CO) phase.

Few experiments are able to discriminate between a homogeneous magnetic state and the averaged magnetic properties of a phase separated state. One of them is Electron Spin Resonance (ESR)⁵. We used this technique recently to probe powder samples of the charge-order compound $\text{Nd}_{0.5}\text{Ca}_{0.5}\text{MnO}_3$, where no trace of the FM phase was detected⁶. In this case, a magnetic field higher than 15 Tesla is required to destroy the CO state in favor of the FM state. The energy difference between the CO phase and the FM phase is too large for the coexistence of both. However, when the compound is in the form of a thin film deposited onto SrTiO_3 or LaAlO_3 substrates, the substrate-induced strain modifies the stability of both phases. In the absence of a magnetic field the slightly incommensurate modulated structure that characterizes the arrangement of Mn^{3+} and Mn^{4+} ions in the CO phase is modified: a smaller incommensurate modulation vector than in the bulk has been observed in $\text{Pr}_{0.5}\text{Ca}_{0.5}\text{MnO}_3$ thin films⁸. Furthermore the critical magnetic field required for the destruction of the CO phase is also strongly reduced as compared to the bulk material: this was illustrated recently in $\text{Pr}_{0.5}\text{Ca}_{0.5}\text{MnO}_3$ thin films^{7,9}. These properties of strained thin films make them good candidates for the occurrence of phase separation and motivated the present

work. We have undertaken an Electron Spin Resonance (ESR) study on 250 nm thick $\text{Pr}_{0.5}\text{Ca}_{0.5}\text{MnO}_3$ thin films (PCMO) grown on LaAlO_3 (LAO). We present strong evidence for a phase separation, with properties depending on the strength and the orientation of the applied magnetic field (H) with respect to the substrate plane (parallel or perpendicular).

II. EXPERIMENTS

PCMO thin films were grown on (100)-LAO substrates using the pulsed laser deposition technique. The details of the experimental procedure are described elsewhere⁸. We have shown that they are single phase, [101]-oriented i.e. with the [101] axis in the $Pnma$ space group being perpendicular to the substrate plane. In the pseudocubic lattice, that will be further used for simplicity, this direction corresponds to one of the quadratic axis i.e. [001]. The out-of-plane lattice parameter, at room temperature, for the 250 nm thick films is 0.384 nm confirming that the PCMO films are under compression in the plane of LAO as previously shown⁹. The stability of the CO phase in the presence of magnetic field was studied by transport measurements⁷. The transition towards the FM phase is shown by the dramatic decrease of the electrical resistivity, the CO phase being insulating while the FM state is metallic. The corresponding phase diagram is given in Figure 1 together with typical magnetoresistance curves. The CO/FM transition as a function of magnetic field is dramatically reduced compared to the bulk when the temperature is lowered. At 150K e.g. it is about 8 Tesla in the film and 15 Tesla in the bulk³. The difference in thermal dilatations between the film and the substrate destabilizes the CO phase. Note also the first order character of the transition evidenced by the hysteresis as previously observed in CO compounds with other compositions¹⁰.

The ESR spectra were recorded at 9.44 GHz using a conventional Bruker spectrometer operating with a 1 Tesla electromagnet. The thin film was cut into a 2x4 mm² plate to avoid cavity saturation, in the paramag-

netic regime at least. For the high field, high frequency measurements, the whole film was used (two $2 \times 4 \text{ mm}^2$ plates superimposed). For these experiments a home-made spectrometer¹¹ was used at frequencies of 95 GHz and 190 GHz with a superconducting magnet operating up to 12 Tesla. The magnetic field was kept below the CO/FM transition (6 Tesla for 95 GHz and 8 Tesla for 190 GHz recorded at 150 K) in order to test the phase separation scenario without passing the first order, hysteretic transition. The high frequency spectrometer uses oversized cylindrical guides for the electromagnetic wave with no cavity at all. This facilitates measurements in the very large frequency range, but the sensitivity is rather poor. Up to four spectra had to be recorded and averaged at each temperature.

III. X BAND MEASUREMENTS

Figure 2 reports on X band spectra for H parallel to the film plane. The spectra were obtained starting from low temperatures. No noticeable change appears with thermal cycling. We checked that the sharp features correspond to the LAO substrate and the signal close to 0.9 Tesla is due to air in the cavity and it disappears under nitrogen pressure. The broad signal at $g = 2.0$ arises from the film itself. It depends strongly on temperature but very weakly on field orientation as can be seen from Figure 3 where the line position B_0 , intensity (proportional to the ESR susceptibility χ) and peak line width ΔB_0 are plotted. Below 150-160K, the line intensity is weakened and deviates markedly from a Lorentzian shape and it finally vanishes. We attribute these effects to the opening of the antiferromagnetic gap and deduce the Néel temperature: $T_N \simeq 140 \text{ K}$, a value lower than the reported value for the bulk (180 K)¹³. The ESR susceptibility follows the general trend of the magnetic susceptibility with a maximum at T_{CO} identified here at $T_{CO} \simeq 240 - 250 \text{ K}$, which corresponds also to the minimum in the ESR linewidth. This value is very close to the one deduced from resistivity measurements on a similar film as well as to the bulk value indicating that T_{CO} does not seem to depend on the film thickness and the substrate-induced stress. However when the temperature is lowered, the changes in cell parameters observed in bulk materials is quenched due to the substrate stress and the CO state has an incommensurate modulated structure⁸. This affects also the magnetic exchange interactions between manganese ions and the antiferromagnetic ordering temperature compared to the bulk is reduced.

The ESR line position B_0 is rather constant in the temperature range 200 K- 300 K. The slight variation as a function of field orientation (6 mT at 200 K) arises from demagnetization effects. The resonant condition is given by $H_{res} = \sqrt{(H_0 + (n_y - n_z)M)(H_0 + (n_x - n_z)M)}$ ¹⁴ where H_0 is the applied magnetic field in the z direction,

M the sample magnetization, $n_{x,y,z}$ the demagnetization factors where the z axis is along the magnetic field direction and H_{res} is the resonance field for a given electromagnetic wave frequency ν : $h\nu = g\mu_B H_{res}$, g is the gyromagnetic factor. Taking the infinite plate geometry and a magnetization $M = 2.10^{-3}\mu_B$ per unit formula at 200 K, the correction for the field applied parallel to the plate is $-2mT$ and for the perpendicular direction $+4mT$. These corrections account well for the discrepancy in line positions for the parallel and perpendicular field directions. We thus conclude that the g factor is equal to 2.02(1) with no crystalline anisotropy.

IV. HIGH FREQUENCY ESR MEASUREMENTS

The high frequency, high field ESR measurements enable us to get more detailed information on the local magnetic order. Spectra recorded at 95 GHz and 190 GHz are presented in figure 4 and 5 for the static field applied parallel to the film plane and in figure 6 for the perpendicular direction. The sharp features at $g = 2.0$ are due to the substrate. Note the decrease in sensitivity as compared to the X band measurements. Nevertheless we are able to detect the manganite film itself which is clearly identified as the broad signal similarly to the X band results. For both field directions, the paramagnetic signal of the CO phase disappears below 130 K due to the opening of the antiferromagnetic gap as already shown in the X band measurements. More surprisingly, another signal is present, which depends on the temperature and the applied magnetic field. For the field parallel to the film plane, this additional signal is on the low field side of the paramagnetic line with the same shift at 95 GHz and 190 GHz (around 0.8T): it is characteristic of a ferromagnetic resonance. It is well defined below 200 K and persists below T_N , revealing the presence of a segregated ferromagnetic phase, weakly coupled to the CO phase. For the field applied perpendicular to the film plane, this additional signal is on the high field side of the paramagnetic line; it is not as well defined and it spreads continuously from the paramagnetic line up to a maximum shift is of about 1.6T. It disappears below T_N , this is expected if the segregated ferromagnetic phase is coupled to the CO phase. In this case the ferromagnetic regions couple to the AF regions and the ferromagnetic resonance mode shifts and broadens if the ferro regions are small.

To model the ferromagnetic resonance, we include in addition to the applied field H_0 , the demagnetization field and the anisotropy field which act on the rotating part of the magnetization induced by the electromagnetic wave. Assuming homogeneous fields within the ferromagnetic regions, we use the concept of demagnetization factors and the resonant condition becomes: $H_{res} = \sqrt{(H_0 + (n_y + n_{ay} - n_z)M)(H_0 + (n_x + n_{ax} - n_z)M)}$ ¹⁴ where $n_{ax,ay}$ denote the fictitious anisotropy constants.

For instance, in a cubic structure with H_0 parallel to one of the cubic axis $n_{ax} = n_{ay} = 2K/M^2$ where M is the ferromagnetic magnetization and K the anisotropy constant. If K is positive, the cubic axis is the easy magnetic axis; if K is negative, it is the hard axis. At high fields, the resonant condition reduces to $H_{res} = H_0 + (n_x + n_y + n_{ax} + n_{ay} - 2n_z)M/2$.

We first consider demagnetization effects. We may assume that the shape of the segregated phase is isotropic in the film plane. Then only one demagnetization factor is needed, $n_{//}$ for instance, which relates to a direction in the film plane. When the field is applied perpendicular to the film, the resonance condition is $H_{res} = H_0 - (1 - 3n_{//})M$. For a measurement at fixed frequency, this leads to a shift $\mu_0\Delta H = \mu_0(1 - 3n_{//})M$. This shift will be positive and maximum for a plate like shape ($n_{//} = 0$ and $\mu_0\Delta H = \mu_0M$); it will be negative for a needle like shape ($n_{//} = 1/2$ and $\mu_0\Delta H = -\mu_0M/2$). The observed shift at 140 K, $\mu_0\Delta H_{obs} = +1.53T$, is positive and even larger than μ_0M (the saturated value at low temperatures is about 0.8T). This is in favor of a plate like shape with an additional shift arising from anisotropy effects. Since $H_0//[001]$ of the pseudo cubic cell, $n_a = 2K/M^2$ and $\mu_0\Delta H = \mu_0(M - 2K/M)$. At 140 K, assuming $\mu_0M = 0.7T$ close to the saturation ferromagnetic value, then $\mu_0H_a = \mu_02K/M = -0.8T$, the same order of magnitude as μ_0M . Such a strong anisotropy field is not usual in manganese perovskites: the corresponding anisotropy constant ($K \simeq -2.10^5 J/m^3$) is 100 times larger than in bulk La(Sr,Pb)MnO₃ crystals¹⁵ and is of opposite sign. In our thin film the FM phase embedded in the CO phase has an enhanced magnetic anisotropy as compared to bulk ferromagnetic samples and contrary to bulk samples the [001] direction is a hard magnetic axis.

For the field applied in the plane of the substrate, $H_{res} = H_0 + (1 - 3n_{//})M/2$ if demagnetization effects alone are taken into account, leading to a shift $\mu_0\Delta H = \mu_0(3n_{//} - 1)M/2$. The observed shift at 140K is $\mu_0\Delta H_{obs} = -0.86T$. The sign of the shift for this field orientation also suggests that the ferromagnetic phase consists of plate like regions with $n_{//} \simeq 0$. Anisotropy effects have to be included here also and these give rise to an additional negative shift: $\mu_0\Delta H = -\mu_0(M + 2K/M)/2$ where K appears to be positive this time. Since the film is twinned in the [010] and [010] directions, a positive anisotropy constant means that both these axis are easy magnetic axis, i.e. the FM phase has an easy plane anisotropy. For an infinitely thin plate like shape, at high fields in the plane, the shift is half that appearing for a field applied perpendicular to the film plane. Figure 7 presents, in a frequency-field diagram, the experimental resonant fields together with the calculated contribution arising from demagnetization effects (assuming a plate like shape for the ferromagnetic phase) and the one arising from anisotropy effects (assuming easy plane anisotropy). A sketch of the segregated ferromagnetic phase is also drawn with the direction of the magnetic easy axis.

Our results should be compared to observations in very thin ferromagnetic films where the strain from the substrate is important^{16,17}. In such cases the positive magnetostriction increases the anisotropy constants: the compressive strain in films grown on LAO substrates results in an out of plane easy magnetic axis while growth on STO substrates, which induces tensile strain, induces an in-plane easy magnetic axis. The enhanced anisotropy of the ferromagnetic phase embedded in the CO phase in our PCMO film can then be understood by the stress induced by the CO phase. Similarly to what happens in thin films, the magnetic anisotropy will be enhanced with larger crystallographic mismatch between the two phases and thinner ferromagnetic layers. The experiments suggest that the FM phase grows in form of thin layers, as was already suggested by the demagnetization effects, and that the FM phase is compressed by the CO phase.

Figure 8 shows the temperature variation of $M + 2|K|/M$ calculated from all the measurements: at 95 GHz and 190 GHz for H_0 parallel to the substrate plane, and at 95 GHz for the perpendicular direction. The different values agree quite well, confirming our model of a plate like shape with easy plane anisotropy. We note a slight increase of $M + 2|K|/M$ with the magnetic field at which the resonance occurs for a given temperature. At higher field, the segregated phase grows, the strain decreases and K becomes smaller. At the same time, the magnetization M increases so that the two effects add. As for the dependence on the field orientation, the segregated phase is much better defined when the field is applied perpendicular to the film plane. This can be seen from the shape of the ESR spectrum arising from the FM phase: it is a well resolved line for the perpendicular direction while it extends continuously from the paramagnetic CO signal for the parallel direction. The latter spectrum indicates a distribution in the shape factor and anisotropy constant. Moreover, the FM line persists at temperatures below the antiferromagnetic transition of the CO phase for the field perpendicular to the film plane, but it disappears below the antiferromagnetic transition for the parallel direction.

Note also that no trace of this segregated phase was detected in the X band measurements on a similar film: this was checked at 200 K and 100 K where we looked at the full angular dependence of the ESR spectrum in the field range 0-1T. This confirms that the amount of this segregated phase depends on the strength of the magnetic field. At fields up to 7T, at 140 K for instance, this FM phase is still a minority phase.

In conclusion, we have shown that a segregated ferromagnetic phase grows within the CO phase in a 250 nm thick PCMO/LAO film. The segregated phase has the shape of very thin layers parallel to the film plane. The segregated domains grow with increasing external field. The segregated FM phase has an enhanced anisotropy constant with an easy plane type of anisotropy. It also depends on the orientation of the applied magnetic field: the segregated phase is better defined for H parallel to the

film. In the perpendicular direction, the ferromagnetic resonance disappears below the antiferromagnetic ordering temperature of the CO phase due to a strong magnetic coupling. This effect may explain why no segregated phase was observed by ESR in LaSrMnO crystals¹⁸, while neutron measurements were able to detect it¹⁹.

We are indebted to J. Dumas for the X band ESR measurements. The Grenoble High Magnetic Field Laboratory is 'laboratoire associé à l'Université Joseph Fourier-Grenoble'. AJ acknowledges the support of the Hungarian state grant OTKA T043255.

* E-mail: sophie@grenoble.cnrs.fr

- ¹ C.N.R. Rao, A. Arulraj, A.K. Cheetham and B. Raveau, *J. Phys.: Condens. Matter.* **12**, R83 (2000).
- ² Y. Tomioka, A. Asamitsu, H. Kuwahara, Y. Moritomo and Y. Tokura, *Phys. Rev. B* **53**, R1689 (1996).
- ³ M. Tokunaga, M. Miura, Y. Tomioka and Y. Tokura, *Phys. Rev. B* **57**, 5259 (1998).
- ⁴ for a review see A. Moreo, S. Yunoki, E. Dagotto, *Science* **283**, 2034 (1999)
- ⁵ O. Chauvet, G. Goglio, P. Molinie, B. Corraze, L. Brohan, *Phys. Rev. Lett.* **81**, 1102 (1998), Run-Wei Li, Zhen-Rong Zhang, Qing-An Li, Ji-Rong Sun, Guang-Jun Wang, Zhi-Hong Wang, Shao-Ying Zhang Bao-Shan Han, Bao-Gen Shen, *J. Appl. Phys.*, **92**, 7404 (2002)
- ⁶ F. Dupont, F. Millange, S. de Brion, A. Janossy, G. Chouteau, *Phys. Rev. B* **64**, R220403 (2001)
- ⁷ W. Prellier, A.M. Haghiri-Gosnet, B. Mercey, Ph. Lecoeur, M. Hervieu, Ch. Simon, B. Raveau, *Appl. Phys Lett.* **77**, 1023 (2000), W. Prellier, E. Rauwel Buzin, Ch. Simon, B. Mercey, M. Hervieu, S. de Brion, G. Chouteau, *Phys. Rev. B* **66**, 024432 (2002)
- ⁸ A.M. Haghiri-Gosnet, M. Hervieu, Ch. Simon, B. Mercey, *J. Appl. Phys.* **88**, 3545 (2000),
- ⁹ W. Prellier, Ch. Simon, A. M. Haghiri-Gosnet, B. Mercey, B. Raveau, *Phys. Rev.* **62**, R16337 (2000)
- ¹⁰ H. Kuwahara, Y. Tomioka, A. Asamitsu, Y. Moritomo and Y. Tokura, *Science* **270**, 961 (1995)
- ¹¹ F. Dupont, S. de Brion, F. Millange, G. Chouteau, *Appl. Magn. reson.* **19**, 485 (2000)
- ¹² A. Biswas, A. Arulraj, A. K. Raychaudhuri and C N R Rao, *J. Phys.: Condens. Matter* **12**, L101 (2000)
- ¹³ M. Tokunaga, N. Miura, Y. Tomioka, Y. Tokura, *Phys. Rev. B* **60**, 6219 (1999)
- ¹⁴ A. Herpin, *Théorie du magnétisme*, Presse Universitaire de France, 1968
- ¹⁵ T.M. Perekalina, I.E. Lipinski, V.A. Timofeeva, S.A. Sherkeyzyan, *Sov. Phys. Solid State* **32**, 1827 (1991)
- ¹⁶ J. O'Donnell, M.S. Rzchowski, J.N. Eckstein, I. Bosovic, *Appl. Phys. Lett.* **72**, 1775 (1998)
- ¹⁷ T.K. Nath, R.A. Rao, D. Lavric, C.B. Eom, L. Wu, F. Tsui, *Appl. Phys. Lett.* **74**, 1615 (1999), X.W. Wu, M.S. Rzchowski, H.S. Wang, Qi Li, *Phys. Rev. B* **61**, 501 (2000)
- ¹⁸ A.A. Mukhin, V. Yu. Ivanov, V.D. Trackin, A. Pimenov, A. Loid, A. Balbadhov, *Europhys. Lett.* **49**, 514 (2000)
- ¹⁹ M. Hennion, F. Moussa, G. Bioteau, J. Rodriguez-Carvajal, L. Pinsard, A. Revcolevschi, *Phys. Rev. B* **61**, 9513 (2000)

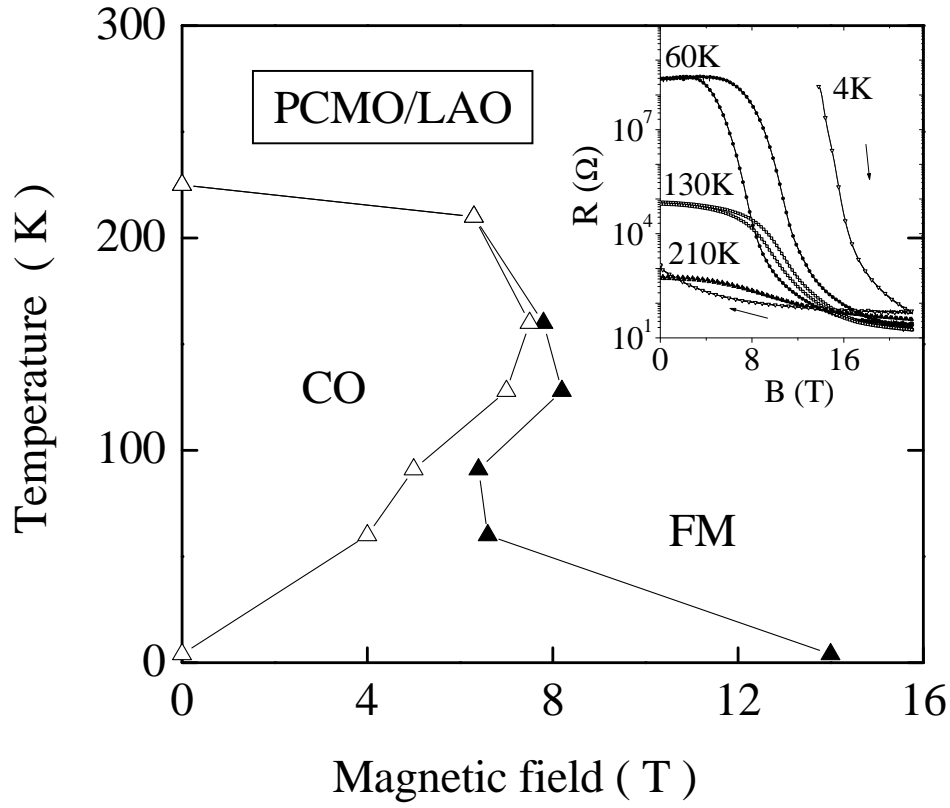


FIG. 1: Temperature, magnetic field phase diagram of a 250 nm thick $\text{Pr}_{0.5}\text{Ca}_{0.5}\text{MnO}_3$ thin film deposited on LaAlO_3 for increasing (▲) and decreasing (△) field. Inset: magnetoresistance curves at different temperatures.

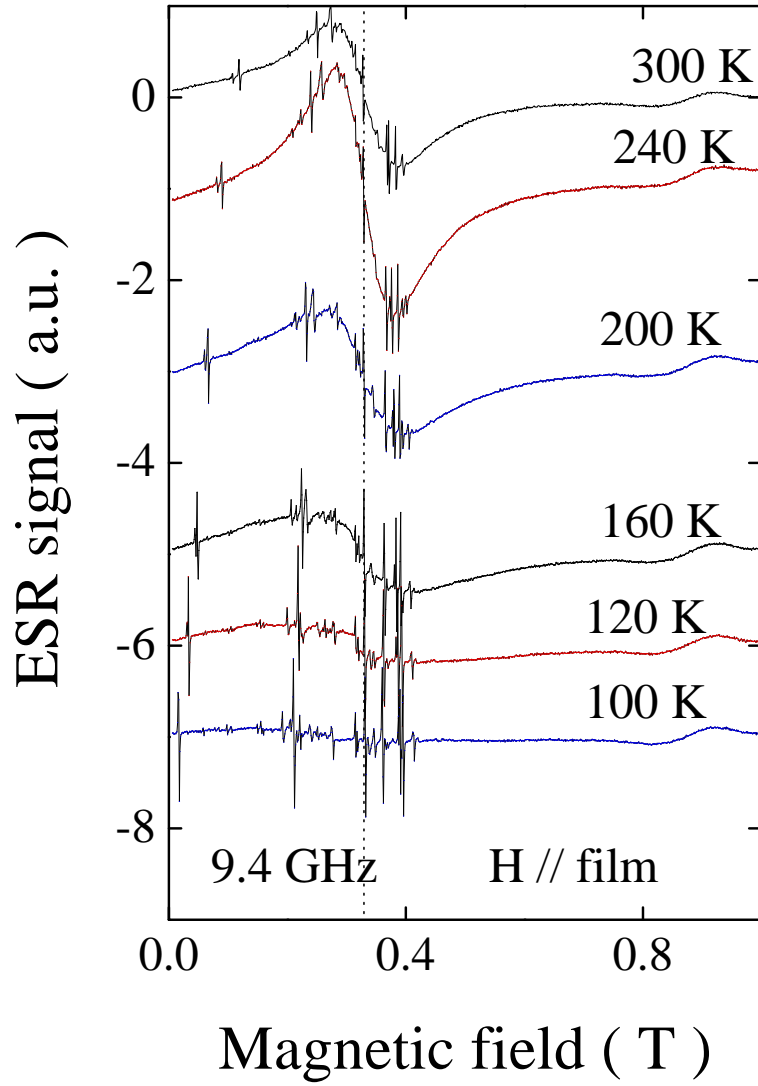


FIG. 2: ESR spectra taken at 9.44 GHz in PCMO/LAO, the static magnetic field was applied parallel to the film plane. The dotted line corresponds to $g=2.00$. The sharp features arise from the LAO substrate and the large signal around $g=2.00$ from the PCMO film.

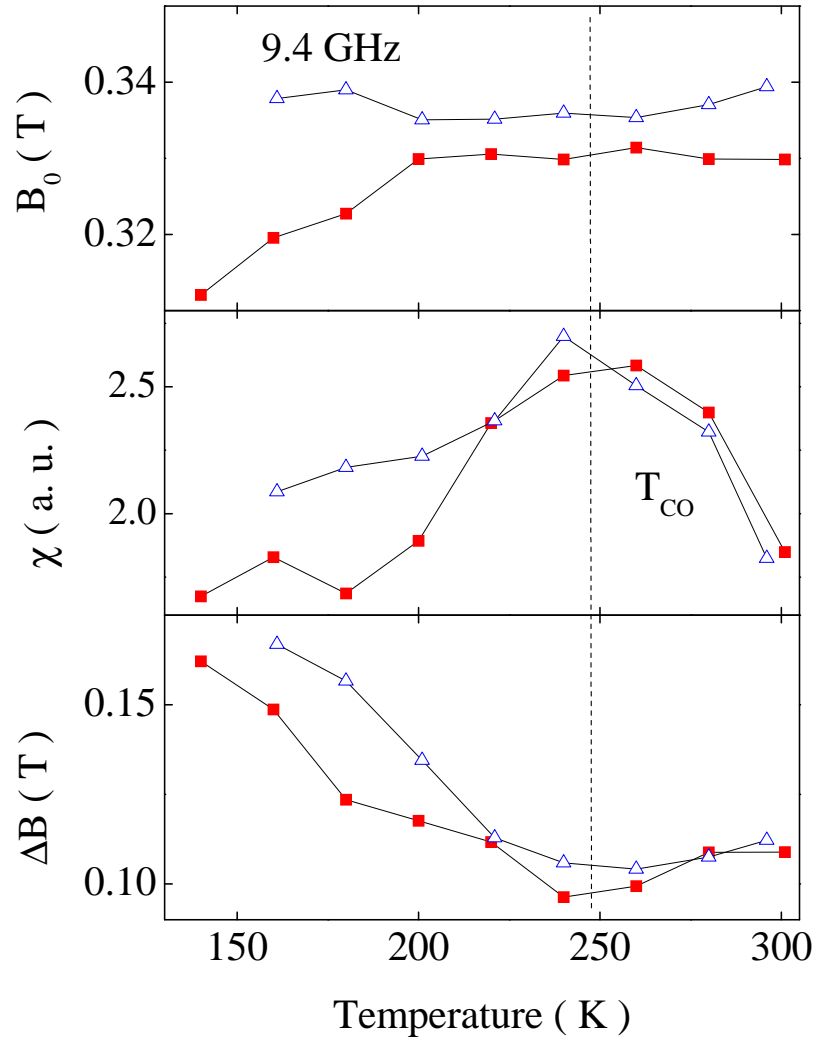


FIG. 3: ESR line position, intensity and line width as a function of temperature in *PCMO/LAO* taken at 9.44GHz for the magnetic field applied parallel (■) and perpendicular (Δ) to the film plane.

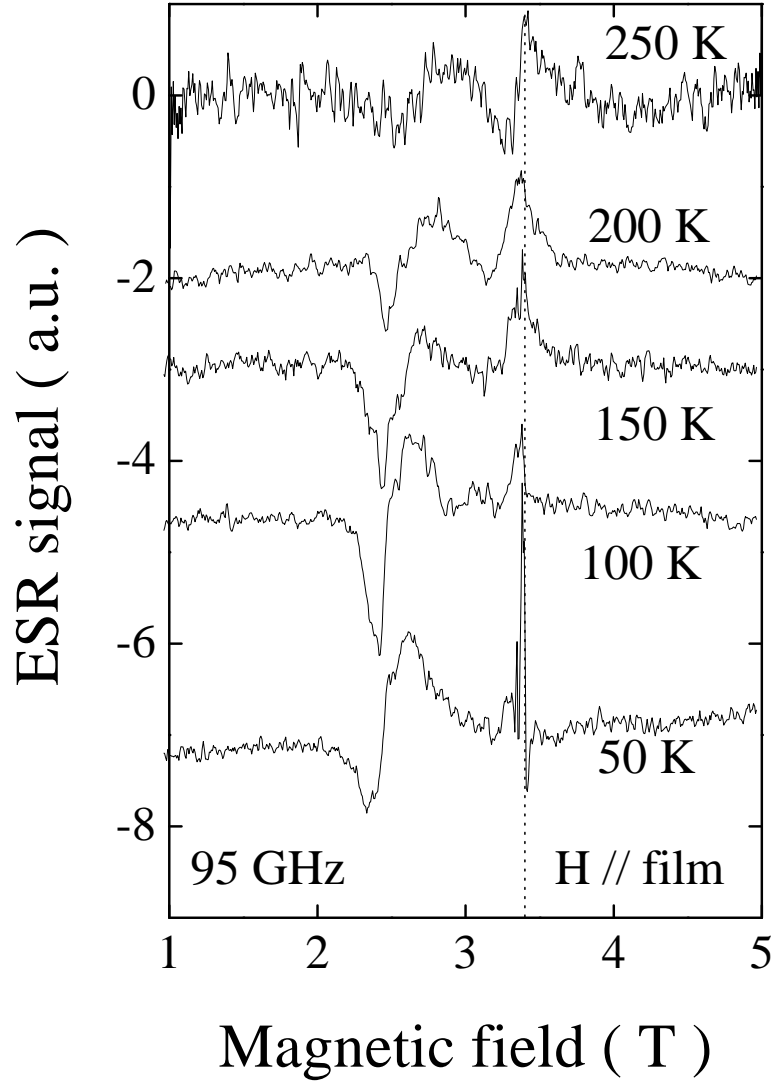


FIG. 4: ESR spectra as a function of magnetic field in *PCMO/LAO* taken at 95GHz and at different temperatures. The magnetic field was applied parallel to the film plane. The dotted line corresponds to $g=2.00$.

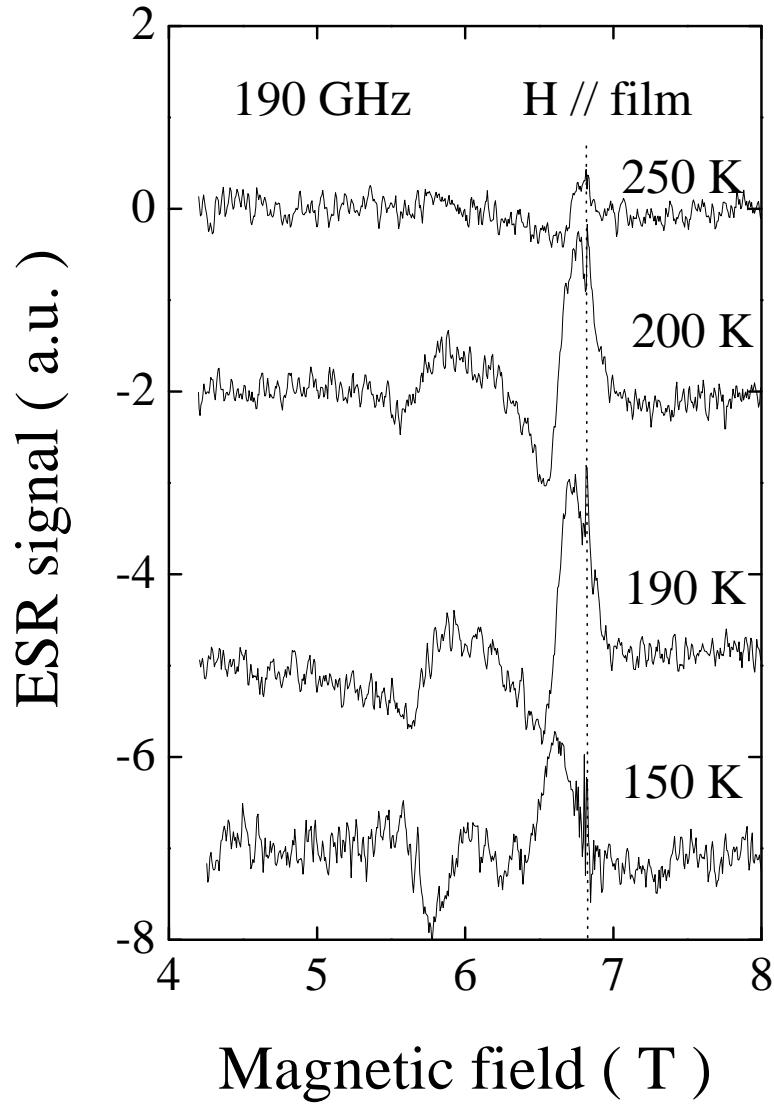


FIG. 5: ESR spectra as a function of magnetic field in *PCMO/LAO* taken at 190GHz and at different temperatures. The magnetic field was applied parallel to the film plane. The dotted line corresponds to $g=2.00$.

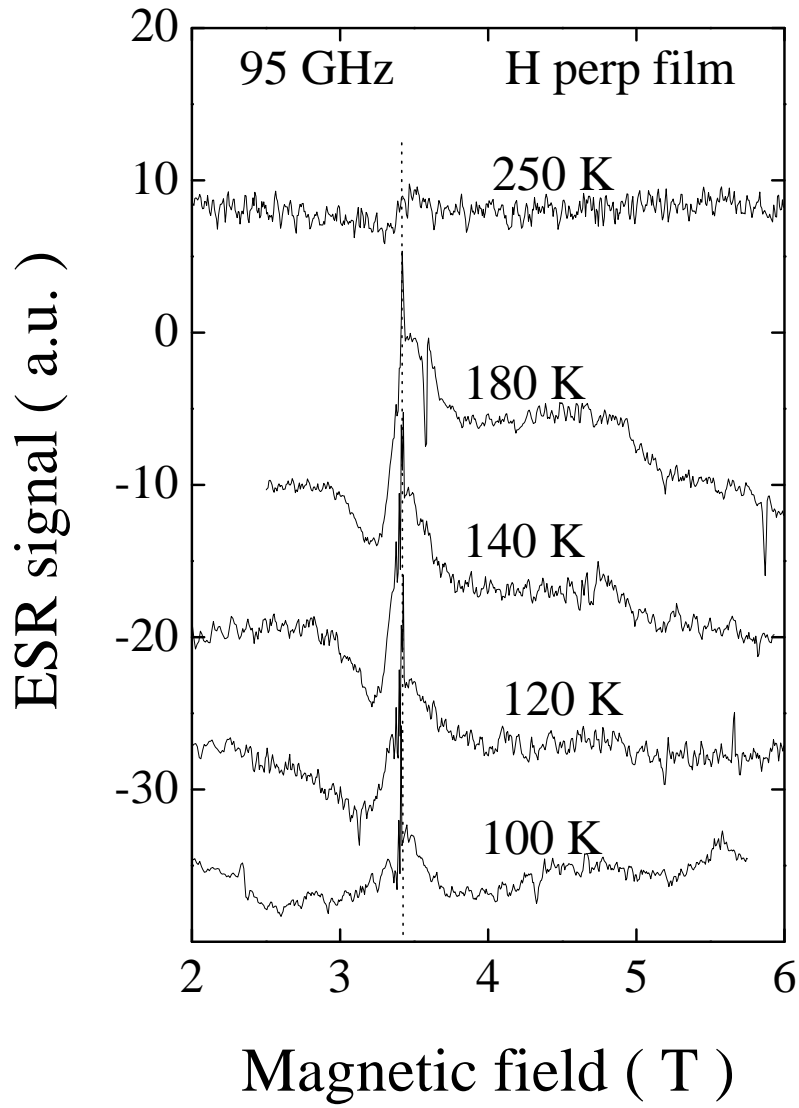


FIG. 6: ESR spectra as a function of magnetic field in *PCMO/LAO* taken at 95GHz and different temperatures. The magnetic field was applied perpendicular to the film plane. The dotted line corresponds to $g=2.00$.

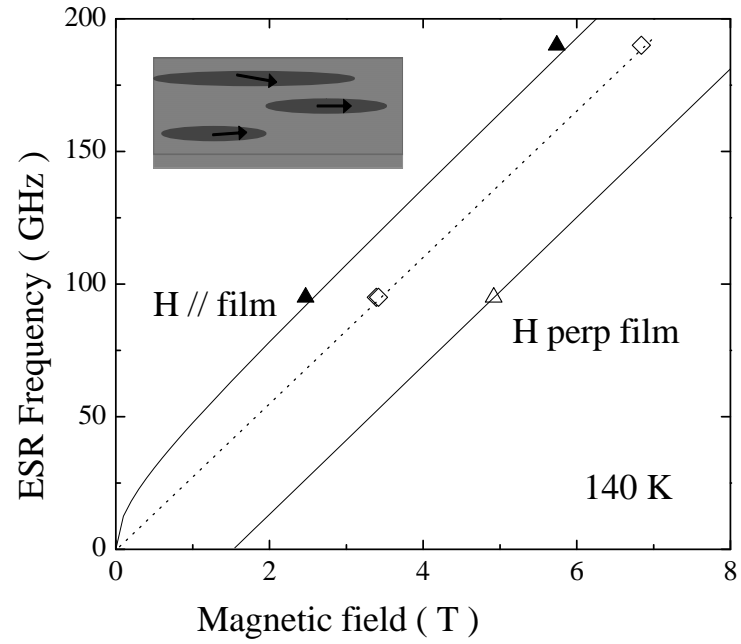


FIG. 7: Ferromagnetic resonance modes in a frequency-field diagram: experimental values at 140K for the magnetic field applied parallel (\blacktriangle) and perpendicular (\triangle) to the film plane and calculated values using the model described in the text (continuous lines). The paramagnetic resonance in the CO phase (\diamond) and calculated (dotted line) are also shown.

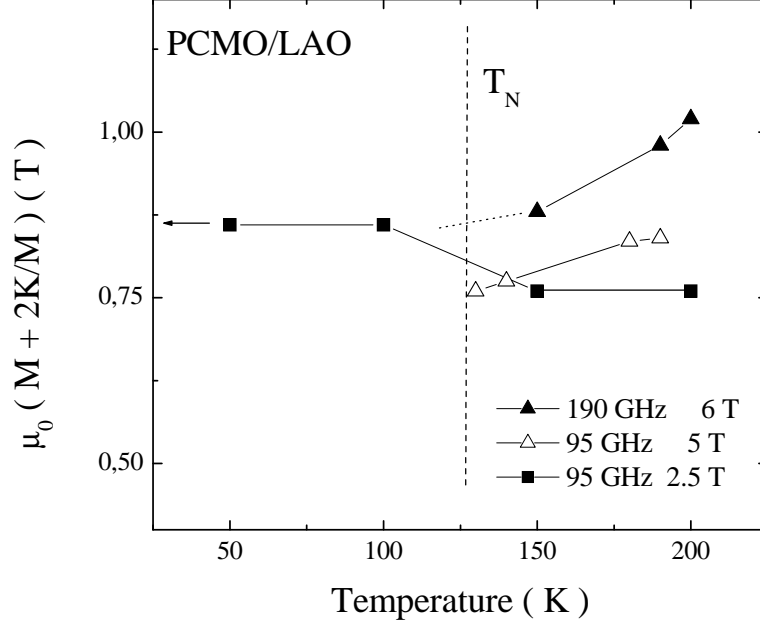


FIG. 8: Temperature dependence of $M + 2|K|/M^2$ calculated from the ESR line shifts (see main text) as a function of temperature for the magnetic field applied parallel (■, ▲) and perpendicular (△) to the film plane.